

BRIEF COMMUNICATION

Nucleocytoplasmic transport defect in a North American patient with ALS8

Robert D. Guber¹, Alice B. Schindler¹, Maher S. Budron¹, Ke-lian Chen¹, Yuebing Li², Kenneth H. Fischbeck¹ & Christopher Grunseich¹¹Neurogenetics Branch, National Institute of Neurological Disorders and Stroke, NIH, 35 Convent Drive, Bethesda, Maryland 20892²Neuromuscular Center, Cleveland Clinic, 9500 Euclid Avenue Cleveland, Ohio 44195**Correspondence**

Christopher Grunseich, Neurogenetics Branch, National Institute of Neurological Disorders and Stroke, NIH, 35 Convent Drive, Bethesda, Maryland 20892.
Tel: 301 402 5423; Fax: 301 480 3365;
E-mail: christopher.grunseich@nih.gov

Funding Information

This work was supported by intramural research funds from the National Institute of Neurological Disorders and Stroke ZIANS003038.

Received: 18 May 2017; Revised: 27 November 2017; Accepted: 29 November 2017

Annals of Clinical and Translational Neurology 2018; 5(3): 369–375

doi: 10.1002/acn3.515

Introduction

Approximately 10% of amyotrophic lateral sclerosis (ALS) cases are familial, and within this group there are mutations in a variety of disease genes with different disease course and manifestations.¹ In 2004, a heterozygous missense mutation (p.P56S) in the gene for vesicle-associated membrane protein-associated protein B (VAPB) was discovered in a large Brazilian motor neuron disease family of Portuguese descent, and this disease was designated ALS8.² Patients presented with manifestations ranging from typical severe ALS with rapid progression to late-onset spinal muscular atrophy.^{2,3} Two other cases of the P56S mutation have since been reported in Germany and China with different founders.^{4,5}

The mechanism by which the P56S VAPB mutation results in motor neuron degeneration is unknown. In overexpression cell models the P56S mutant protein is mislocalized and coaggregated with the wild-type VAPB.⁶

Abstract

Amyotrophic lateral sclerosis 8 (ALS8) is a rare progressive neurodegenerative disease resulting from mutation in the gene for vesicle-associated membrane protein-associated protein B. We evaluated a North American patient using exome sequencing, and identified a P56S mutation. The disease protein had similar subcellular localization and expression levels in the patient and control fibroblasts. Patient fibroblasts showed increased basal endoplasmic reticulum stress and dysfunction of nucleocytoplasmic transport as evidenced by impaired Ran trafficking. This finding extends the identification of ALS8 into North America, and indicates a cellular defect similar to other forms of hereditary motor neuron disease.

However, an ALS8 motor neuron cell model was found to have reduced levels of the P56S mutant protein without mislocalization.⁷ Some studies have shown that mutant VAPB results in endoplasmic reticulum (ER) stress, and unfolded protein response (UPR) activation, while other studies have shown a loss of IRE1a activated UPR with the P56S mutation.^{6,8,9} The effects of P56S mutation on ER stress and UPR activation remains to be further defined in patient cells.

Transfection of P56S VAPB has previously been shown to disrupt the nuclear envelope.¹⁰ An SOD1 transgenic mouse model of ALS displayed defects in importin transport proteins in the anterior horn, indicative of a nucleocytoplasmic transport defect in ALS.¹¹ Disruption of nucleocytoplasmic transport system has also been described in familial ALS due to C9orf72 repeat expansion.^{12,13} More specifically, Ras-related nuclear protein (Ran) GTPase is mislocalized to the cytoplasm in C9orf72 cells.¹³ In this study, we have identified a similar

disruption of nucleocytoplasmic transport in ALS8. We describe here the first reported case of ALS8 mutation in North America. Through study of patient fibroblasts, we show increased basal levels of ER stress and impairment of Ran transport.

Materials and Methods

Clinical characterization and diagnosis

The study was performed with approval from the NIH Combined Neuroscience (CNS) Institutional Review Board, and informed consent was obtained. The subject was evaluated at the NIH Clinical Center and skin fibroblasts were obtained from the forearm by punch biopsy. Whole-exome sequencing was performed on DNA extracted from whole blood using the NimbleGen SeqCap EZ Ver. 3.0 + UTR capture kit. For haplotype analysis, genomic TUBB1 sequence was performed with Sanger sequencing (Table S1).

Immunoblotting and reverse transcription-quantitative PCR (RT-qPCR)

Fibroblasts were grown in high-glucose DMEM with 10% FBS, and 1% penicillin-streptomycin-glutamine. Fibroblast lysates were evaluated by immunoblotting with the antibodies listed in Table S2. Three replicates were analyzed from different cell culture passages. Densitometric analysis was performed using ImageJ (NIH). Total RNA was extracted from fibroblasts using TRIzol Reagent per manufacturer recommendations (ThermoFisher Scientific). qPCR reactions were run using SYBR green master mix (ThermoFisher Scientific) with primers listed in Table S1 using an average of three replicates for each sample from one culture of fibroblasts.

Immunohistochemistry

Fibroblasts were stained on coverslips as previously described.¹⁴ Antibodies used for staining can be found in Table S2. Image quantification of the nuclear-to-cytoplasmic ratio of Ran, and nuclear TDP-43 was performed with ImageJ. All image analyses were performed blinded. Fibroblasts transfected with Ran-GFP plasmid RG208738 (Origene) were collected after 24 h.

Statistical analysis

Two-tailed Student *t*-tests were used for statistical analysis.

Results

Clinical evaluation

The index patient, of reported Northern European ancestry, presented at age 37 with a 6-year history of progressive weakness requiring a wheelchair. On examination, he was found to have distal weakness, atrophy, and hyperreflexia. He had a family history of neuromuscular illness in that his mother, aunt, and maternal grandmother had been similarly affected (Fig. 1A). Exome sequencing of whole blood DNA identified a heterozygous mutation in VAPB, P56S, which was further confirmed in cultured fibroblasts (Fig. 1B). The mutation lies within the major sperm domain region of the protein (Fig. 1C).² Analysis of a nearby TUBB1 3' UTR polymorphism (rs10485828) indicated that the patient did not carry the C allele segregating with the mutation in the Brazilian families.^{2,4}

VAPB P56S mutation results in ER stress

We did not observe any difference in the localization and total protein levels of the P56S mutant VAPB compared to wildtype (Fig. 2A). We investigated whether ER stress and UPR activation result from the P56S mutant. Total levels of the UPR sensor PKR-like ER kinase (PERK) were significantly elevated in the ALS8 fibroblasts compared to control (Fig. 2B). We found a significant increase in the expression of genes associated with early stage PERK pathway activation, including CHOP and ATF4, the related chaperones ERDJ4 and DNAJC3, and the spliced form of XBP1, a member of the IRE1a branch of UPR (Fig. 2C). These data show that there is increased basal ER stress and UPR activation in the ALS8 fibroblasts.

Nucleocytoplasmic impairment in ALS8 fibroblasts

We investigated whether the mutation in VAPB protein results in abnormal nucleocytoplasmic trafficking of Ran and TDP-43. ALS8 fibroblasts had a significant decrease in the ratio of endogenous Ran in the nucleus relative to the cytoplasm compared to control cells (Fig. 3A and B), and a similar pattern was found upon transfection with Ran-GFP fusion protein (Fig. S1). To further characterize the abnormality in Ran localization, we investigated Ran GTPase Activating Protein 1 (RanGAP1) SUMOylation, which occurs at the nuclear envelope, and found it to be significantly decreased in the ALS8 fibroblasts (Fig. 3C). We further investigated TDP-43 localization and found a significant decrease in nuclear TDP-43 in the ALS8 fibroblasts compared to control (Fig. 3D and E). These

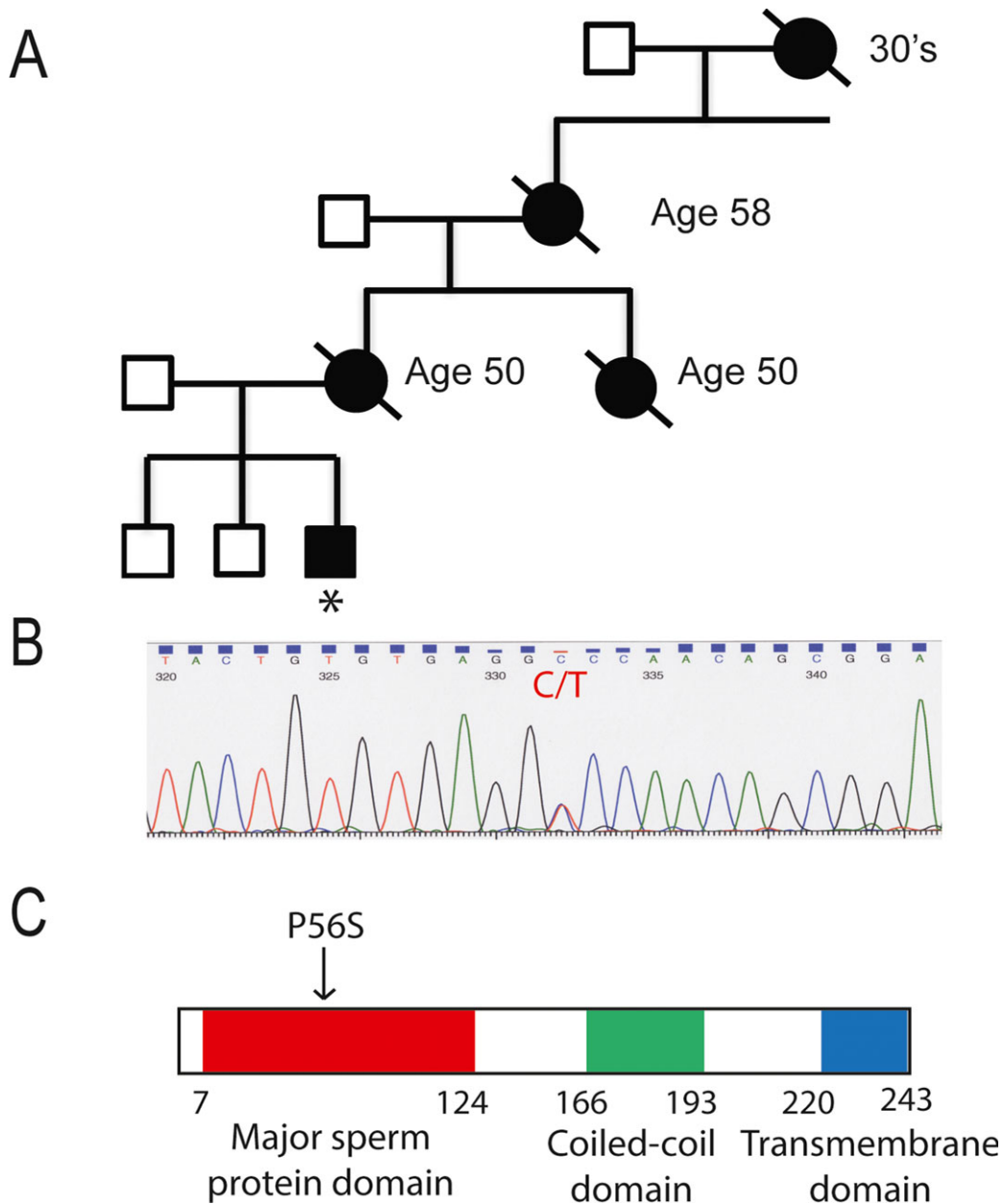


Figure 1. ALS8 pedigree and mutation. (A) Pedigree of affected family members. The patient described in this study is labeled with an asterisk. (B) DNA sequence chromatogram of the affected family member’s fibroblasts confirming the exome sequencing result. The heterozygous C to T peak is indicated. (C) Primary structure of vesicle-associated membrane protein-associated protein B showing the location of the ALS8 mutation at codon 56.

findings indicate that there is a defect in Ran nucleocytoplasmic trafficking in the ALS8 patient cells.

Discussion

Here, we report a North American ALS8 patient with normal expression of VAPB, molecular features of basal ER stress, UPR activation, and impairment of

nucleocytoplasmic transport. The P56S mutation has been previously reported in Brazil, Germany, and China. The patient described here had features of both upper and lower motor neuron disease in a pattern consistent with previous reported findings.^{3–5}

VAPB is known to be localized to the ER, and the P56S mutant protein aggregates into inclusions resulting in altered ER structure.^{6,15,16} We did not detect any

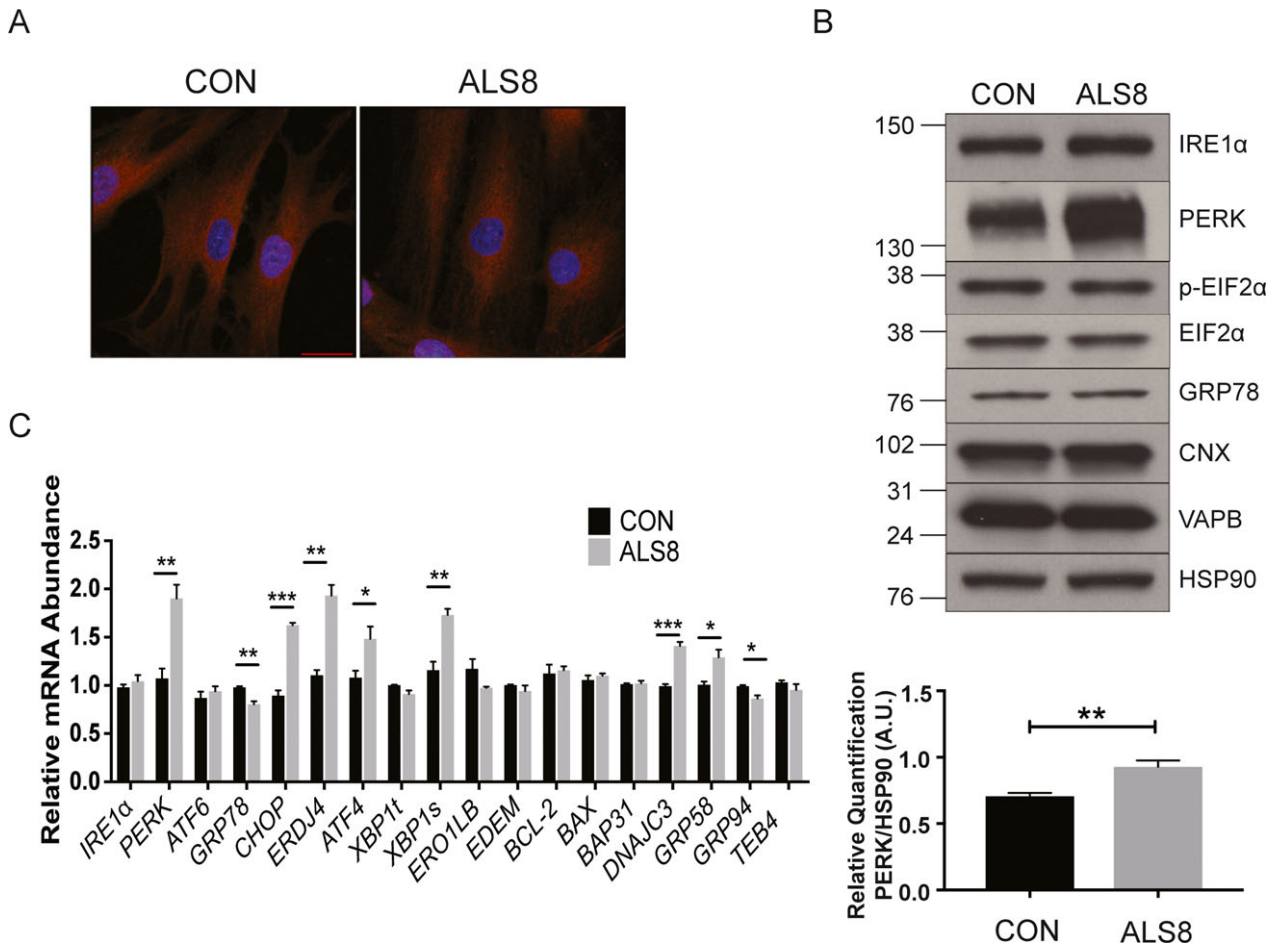


Figure 2. Basal ER stress in ALS8 patient fibroblasts. (A) Control and ALS8 patient fibroblasts stained with VAPB (red) and DAPI (blue). Scale bar = 25 μm. There is no difference in VAPB staining from 10 fields of view evaluated. (B) Immunoblot analysis of ER stress, UPR proteins, and VAPB protein. VAPB levels are normal, and PERK is significantly increased. HSP90 was run as a loading control. Quantification of PERK to HSP90 is shown below. Data are mean ± SEM of 3 technical replicates. ***P* < 0.01. (C) qPCR analysis of UPR and VAPB related genes. XBP1 total (XBP1t) and XBP1 spliced (XBP1s). Data are mean ± SEM of three technical replicates. **P* < 0.05, ** *P* < 0.01, ****P* < 0.001. VAPB, vesicle-associated membrane protein-associated protein B; UPR, unfolded protein response; ALS8, amyotrophic lateral sclerosis 8.

difference in the localization or amount of mutant VAPB compared to control, consistent with previous observations in patient cells.⁷ We used cells with a physiologically appropriate level of VAPB expression, in contrast to earlier studies with overexpression models which showed decreased levels of soluble mutant protein.⁹

The mechanism by which the P56S VAPB mutation results in ER stress is still unknown, however, this study provides evidence for the association between increased basal ER stress, UPR activation with PERK activation and splicing of XBP1. Previous studies have reported decreased UPR activity with the P56S mutation, while other models have shown activation of the UPR.^{6,8,9} Our results contrast with studies done in overexpression cell models where the VAPB mutation was found to result in the reduced activation of UPR (IRE1a and ATF6).^{6,9} In

transgenic mouse models of P56S, there was evidence of increased ER stress, as we saw in patient cells.^{8,17} The mRNA expression profile in our patient showed a pattern indicative of ER stress, with an increase in chaperones, PERK pathway genes, and spliced XBP1, as has been reported in other disease models.^{18,19} Induction of ER stress and the UPR could protect the cells from protein misfolding and dysfunction caused by the P56S mutation. We did not find an increase in TEB4 expression in the ALS8 fibroblasts, which may indicate that the mutant protein is cleared from the ER. It will be important to understand the mechanism of clearance of P56S from the ER, and the balance between UPR and protein degradation in the disease.

Previous studies have shown decreased interaction of P56S mutant VAPB with the nuclear envelope,¹⁰ an

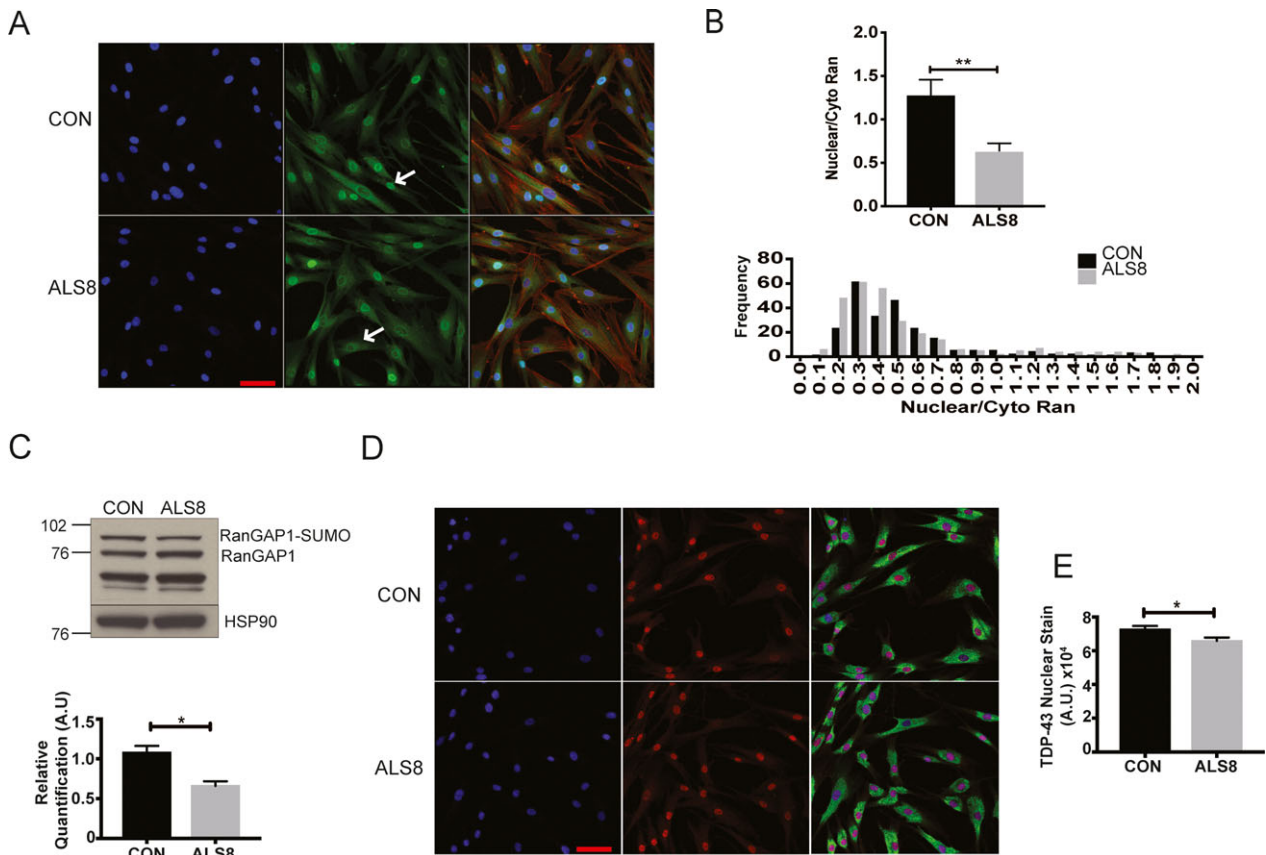


Figure 3. Impairment of nucleocytoplasmic transport in ALS8. (A) Control and ALS8 patient fibroblasts stained with Ran (green), phalloidin (red) to display the cytoplasm, and DAPI (blue) to identify the nuclei. Arrows show the increased nuclear (control) and cytoplasmic (ALS8) Ran staining. Heterogeneity of Ran localization was detected in all fields of view. Scale bar is 50 μm . (B) Quantification of the nuclear to cytoplasmic Ran gradient in control and ALS8 fibroblasts. The ratio represents 11 fields of view with 271 fibroblasts counted for each. The graph represents the mean \pm SEM. The histogram represents the cell distribution of nucleocytoplasmic Ran gradient, displaying a lower ratio (more cytoplasmic Ran) in the ALS8 fibroblasts. The bars represent cell counts. $**P < 0.01$. (C) Immunoblot analysis of RanGAP1-SUMO and RanGAP1 (non-SUMO). HSP90 is used as a loading control. Relative quantification shown of RanGAP1-SUMO to the non-SUMO (cytoplasmic) form. Data are mean \pm SEM. $*P < 0.05$, $n = 3$. (D) Control and ALS8 patient fibroblasts stained with Protein Disulfide Isomerase (green) to show the cytoplasm, TDP-43 (red), and DAPI (blue) to identify the nuclei. Scale bar is 50 μm . (E) Quantification of the nuclear TDP-43 intensity in control and ALS8 fibroblasts. The ratio represents 12 fields of view for each with 259 fibroblasts counted for control and 255 fibroblasts counted for ALS8. The graph shows the mean \pm SEM. $*P < 0.05$. ALS8, amyotrophic lateral sclerosis 8.

alteration that led us to investigate whether nucleocytoplasmic trafficking is affected in the ALS8 patient fibroblasts. Disruption of the Ran GTPase-mediated nucleocytoplasmic transport has been of interest since it was found to be disrupted in SOD1 and C9orf72 ALS.^{11–13,20} In the ALS8 patient cells we found abnormal Ran distribution with increased cytoplasmic localization. We further investigated the abnormal localization and identified a decrease in the SUMOylated form of RanGAP1. RanGAP1 helps to accelerate the GTP hydrolysis function of Ran GTPase, converting Ran-GTP to Ran-GDP and promoting the activation of import carriers.²¹ The loss of SUMOylation of RanGAP1 likely results in the loss of localization at the nuclear pore complex and loss of

function of RanGAP1.^{22,23} We also found a decrease in nuclear TDP-43 in the ALS8 fibroblasts. It was previously shown that there is a correlation between the cytoplasmic localization of Ran and TDP-43 indicating the relationship between defects in these pathways.²⁴ Previous studies have shown decreased interaction of P56S mutant VAPB with the nuclear envelope,¹⁰ an alteration that may be leading to a defect in nucleocytoplasmic trafficking. Our results suggest the misfolded VAPB may be resulting in dysfunction in two compartments of the cell, the nuclear pore complex by altering the SUMOylation of RanGAP1, and the endoplasmic reticulum by activating the UPR. This finding provides a mechanistic link between ALS8 and other forms of familial ALS.

In conclusion, we identified a North American patient with ALS8. We found evidence of ER stress under basal conditions in patient fibroblasts. Finally, we provide insight into a common mechanism in familial ALS through the disruption of nucleocytoplasmic transport and abnormal cytoplasmic localization of Ran in ALS8.

Acknowledgments

The authors thank the research subject who made this study possible, and Elizabeth Hartnett and the clinical staff of the NIH neurology clinic for their help with the subject's visit. The authors also thank the NIH Intramural Sequencing Center (NISC) for whole-exome sequencing. We also thank Dr. Haubin Cai (NIA) for the hVAPB antibody. This work was supported by intramural research funds from the National Institute of Neurological Disorders and Stroke.

Author Contributions

R.D.G. and C.G. designed the study. A.B.S., Y.L., R.D.G., and C.G. did the patient evaluations. R.D.G., K.C., M.S.B., and C.G. performed the experiments. R.D.G., K.H.F., and C.G. interpreted the data and drafted the manuscript.

Conflict of Interest

None declared.

References

1. Taylor JP, Brown RH, Cleveland DW. Decoding ALS: from genes to mechanism. *Nature* 2016;539:197–206.
2. Nishimura AL, Mitne-Neto M, Silva HCA, et al. A mutation in the vesicle-trafficking protein VAPB causes late-onset spinal muscular atrophy and amyotrophic lateral sclerosis. *Am J Hum Genet* 2004;75:822–831.
3. Nishimura AL, Al-Chalabi A, Zatz M. A common founder for amyotrophic lateral sclerosis type 8 (ALS8) in the Brazilian population. *Hum Genet* 2005;118:499–500.
4. Funke AD, Esser M, Krüttgen A, et al. The p. P56S mutation in the VAPB gene is not due to a single founder: the first European case. *Clin Genet* 2010;77:302–303.
5. Di L, Chen H, Da Y, et al. Atypical familial amyotrophic lateral sclerosis with initial symptoms of pain or tremor in a Chinese family harboring VAPB-P56S mutation. *J Neurol* 2016;263:263–268.
6. Suzuki H, Kanekura K, Levine TP, et al. ALS-linked P56S-VAPB, an aggregated loss-of-function mutant of VAPB, predisposes motor neurons to ER stress-related death by inducing aggregation of co-expressed wild-type VAPB. *J Neurochem* 2009;108:973–985.
7. Mitne-Neto M, Machado-Costa M, Marchetto MCN, et al. Downregulation of VAPB expression in motor neurons derived from induced pluripotent stem cells of ALS8 patients. *Hum Mol Genet* 2011;20:3642–3652.
8. Aliaga L, Lai C, Yu J, et al. Amyotrophic lateral sclerosis-related VAPB P56S mutation differentially affects the function and survival of corticospinal and spinal motor neurons. *Hum Mol Genet* 2013;22:4293–4305.
9. Kanekura K, Nishimoto I, Aiso S, Matsuoka M. Characterization of Amyotrophic Lateral Sclerosis-linked P56S Mutation of Vesicle-associated Membrane Protein-associated Protein B (VAPB/ALS8). *J Biol Chem* 2006;281:30223–30233.
10. Tran D, Chalhoub A, Schooley A, et al. A mutation in VAPB that causes amyotrophic lateral sclerosis also causes a nuclear envelope defect. *J Cell Sci* 2012;125:2831–2836.
11. Zhang J, Ito H, Wate R, et al. Altered distributions of nucleocytoplasmic transport-related proteins in the spinal cord of a mouse model of amyotrophic lateral sclerosis. *Acta Neuropathol* 2006;112:673–680.
12. Freibaum BD, Lu Y, Lopez-Gonzalez R, et al. GGGGCC repeat expansion in C9orf72 compromises nucleocytoplasmic transport. *Nature* 2015;525:129–133.
13. Zhang K, Donnelly CJ, Haeusler AR, et al. The C9orf72 repeat expansion disrupts nucleocytoplasmic transport. *Nature* 2015;525:56–61.
14. Grunseich C, Zukosky K, Kats IR, et al. Stem cell-derived motor neurons from spinal and bulbar muscular atrophy patients. *Neurobiol Dis* 2014;70:12–20.
15. Gkogkas C, Middleton S, Kremer AM, et al. VAPB interacts with and modulates the activity of ATF6. *Hum Mol Genet* 2008;17:1517–1526.
16. Fasana E, Fossati M, Ruggiano A, et al. A VAPB mutant linked to amyotrophic lateral sclerosis generates a novel form of organized smooth endoplasmic reticulum. *FASEB J* 2010;24:1419–1430.
17. Bertolotti A, Zhang Y, Hendershot LM, et al. Dynamic interaction of BiP and ER stress transducers in the unfolded-protein response. *Nat Cell Biol* 2000;2:326–332.
18. van Galen P, Kreso A, Mbong N, et al. The unfolded protein response governs integrity of the haematopoietic stem-cell pool during stress. *Nature* 2014;510:268–272.
19. Sun S, Shi G, Han X, et al. Sel1L is indispensable for mammalian endoplasmic reticulum-associated degradation, endoplasmic reticulum homeostasis, and survival. *Proc Natl Acad Sci USA* 2014;111:E582–E591.
20. Nagara Y, Tateishi T, Yamasaki R, et al. Impaired cytoplasmic-nuclear transport of hypoxia-inducible factor-1 α in amyotrophic lateral sclerosis. *Brain Pathol* 2013;23:534–546.
21. Bischoff FR, Klebe C, Kretschmer J, et al. RanGAP1 induces GTPase activity of nuclear Ras-related Ran. *PNAS* 1994;91:2587–2591.

22. Evdokimov E, Sharma P, Lockett SJ, et al. Loss of SUMO1 in mice affects RanGAP1 localization and formation of PML nuclear bodies, but is not lethal as it can be compensated by SUMO2 or SUMO3. *J Cell Sci* 2008;121:4106–4113.
23. Zhang H, Saitoh H, Matunis MJ. Enzymes of the SUMO modification pathway localize to filaments of the nuclear pore complex. *Mol Cell Biol* 2002;22:6498–6508.
24. Ward ME, Taubes A, Chen R, et al. Early retinal neurodegeneration and impaired Ran-mediated nuclear import of TDP-43 in progranulin-deficient FTLD. *J Exp Med* 2014;211:1937–1945.

Supporting Information

Additional Supporting Information may be found online in the supporting information tab for this article:

Figure S1. Impairment of nucleocytoplasmic transport in ALS8 fibroblasts.

Table S1. List of primers.

Table S2. List of antibodies.